INTEGRATION OF AIRBORNE HYPERSPECTRAL IMAGERY AND AIRBORNE LIDAR POINT CLOUDS FOR OBJECT-BASED CLASSIFICATION

Chun-Hsuan Huang[1], Tee-Ann Teo[2]
[1] Master Student, Dept. of Civil Engineering, National Chiao Tung University, Hsinchu, Taiwan 30010.
E-mail: rick84032@gmail.com
[2] Associate Professor, Dept. of Civil Engineering, National Chiao Tung University, Hsinchu, Taiwan 30010.
E-mail: tateo@mail.nctu.edu.tw

KEY WORDS: hyperspectral, lidar, data integration, ground classification

ABSTRACT: Remote sensing technologies obtain spectral and shape properties of ground objects efficiently. These useful information is suitable for land use management. The hyperspectral image provides more detail of spectral information and there is a great potential to identify species of vegetation using hyperspectral image. Moreover, lidar data provides 3-D surface to identify different objects on the ground. Hence, the aim of this study is to integrate the hyperspectral imagery and lidar feature for object-based classification. The object-based classification uses image segmentation to produce image objects. Different object's features are calculated from hyper spectral image and lidar data for image classification. The proposed scheme includes image segmentation, feature selection, and image classification. In image segmentation, the image is segmented into image objects from pixels. According to the characteristic of image objects, appropriate features are selected for analysis. In feature selection, nearest neighbor method is used to classify the image at image classification step. In the study, the airborne hyperspectral image and lidar point clouds are collected by ITRES CASI-1500 and Optech ALTM Pegasus. The confusion matrix is generated by ground truth information. The verification includes the comparison between pixel-based and object-based classifications, comparison between multispectral and hyperspectral image classifications, and image classification with and without lidar features. The experimental results indicate that the fusion of hyperspectral image and lidar point clouds may improve the accuracy of image classification. In summary, hyperspectral image provide useful spectral information while lidar data provide useful shape information. The integration of these two data may separate different land covers from both spectrum and geometric information.

1. INTRODUCTION

Due to the technological and environmental development, human living space is expanding rapidly and globally. Hence, land use management is one of the important issues in climate change. The remote sensing technologies obtain useful information of land cover effectively. It can be used to understand different land covers for environment management.

Hyperspectral image provides detailed spectral information. According to the results of classification provided by previous studies (Ifarraguerri and Chang,2000; Shaw and Manolakis,2002; Miao et al.,2006; Prasad and Bruce,2008; Xing et al.,2005), hyperspectral image has a great potential to identify species of vegetation using spectral information. Moreover, with the development of lidar technology, lidar obtains high density 3-D point cloud rapidly. This lidar point clouds provide 3-D surface information efficiently, and this 3-D surface information can use to assist the identification of land cover (Gou et al., 2011), because every ground object has its own characteristic of height. Therefore, the integration of hyperspectral and lidar is beneficial in land cover classification.

The image classification includes pixel-based and object-based classifications (Myint et al, 2011; Duro et al., 2012; Zhang and Xie, 2012). The pixel-based classification analyzes attribute value by pixel. This method does not consider the relation between pixels. Therefore, object-based classification is used in this study. Through the image segmentation, the related image pixels are combined into image objects. The image object provides not only attribute value but factor of shape to identify the class of ground surface (Ke et al., 2010). The aim of this study is to integrate the hyperspectral imagery and lidar feature for object-based classification, and discuss effectiveness of data integrate and object-based classification.

2. MATERIALS

2.1 Study area

The test area is located in the junction of Chiaya and Kaohsiung in Taiwan and the total area is about 21.4 square kilometers. It is a mountainous area which has different types of vegetation, for example, bamboo, fruit, etc. This area also covers some villages and some mountainous regions are developed as farming land and orchard.

Figure 1. The location of study area (red area)

2.2 Hyperspectral image

The hyperspectral image in this study is collected from ITRES CASI 1500. Total numbers of the image bands are 72 bands, and spectral wavelength range is from 362.8nm to 1051.3 nm. The preprocessing of hyperspectral image includes radiation and geometric correction. In order to get the same ground surface reflectivity of every strip, ATCOR4 method is used to the radiation correction, this method consider variety of factors include incident angle, terrain effects and atmospheric effects, and decrease effects from these reason. Furthermore hyperspectral image has a large number of bands, in order to avoid curse of dimensionality in limited training area, the minimum noise fraction transformation (MNF) method is used to reduce dimensions of hyperspectral image. Seven MNF's bands are selected for classification.

2.3 Lidar data

The lidar data is collected by Optech ALTM Pegasus. In order to integrate the lidar and hyperspectral image, lidar is interpolated to 2D raster grid. The features of lidar include nDSM, roughness, intensity and echo ratio. In lidar data processing, point clouds are classified into ground points and non-ground points for digital terrain model (DTM) and the digital surface model (DSM). The DSM can be used in the process of image ortho-rectification, also the normalized digital surface model (nDSM) can be calculated by subtracting the DSM from DTM. Furthermore, standard deviation of DSM can be treated as surface roughness. For lidar signal features, the echo ratio parameterizes multiple reflections, using to represent extension and transparency in vertical, because the region of vegetation has high extension and transparency, this feature can be used to identify vegetation (Höfle and Hollaus, 2010). The intensity means a relative measure for each lidar signal, this information can use for distinguishing ground object and tree species by reflection characteristics (Kim et al., 2009).

3. METHODOLOGY

The work flow of classification is shown as figure 2. First, the purpose in data preprocessing is co-registration, therefore, lidar data and hyperspectral image are registered correctly for classification. Second, setting the land types for classification, according to simple image interpretation the targets of classification are decided. Then, the favorable features are extracted for targets. In object-based classification step include three parts as segmentation, training and classification. Finally, the result of classification has analyzed.

3.1 Set targets of classification

According to the characteristics of test area and recognizable features, this area is roughly divided into vegetation and non-vegetation. The non-vegetation included bare ground, river and various types of man-made structures. The vegetation includes forest, grass and various types of crops. The details of land cover are defined in Table 1.

3.2 Feature extraction

The feature extraction is to produce feature for classification from hyperspectral image and lidar data. Hyperspectral image mainly provides spectral feature while lidar data mainly provides terrain feature and lidar signal features. These features for classification are shown as Table 2.

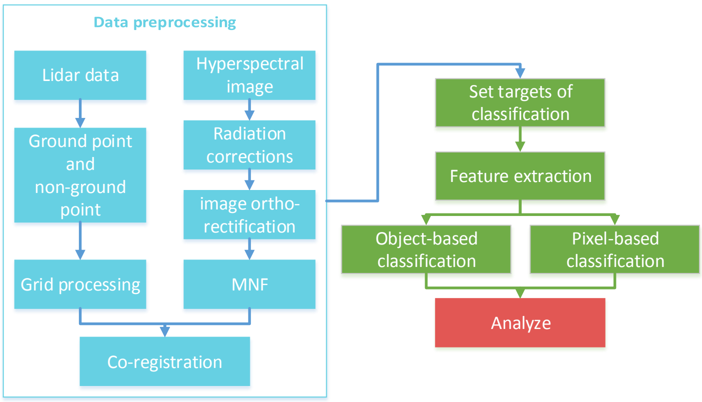

Figure 2. Workflow

Table 1. Targets of classification

Vegetation		Non-vegetation	
1.Broadleaf forest(forest)	5.Bamboo	8.Water	12.Watercourse
2.Grass	6.Fruit tree(fruit)	9.Road	13.Bare ground
3.Tea plantation(Tea)	7.Areca plantation(Areca)	10Greenhouse	14.Concrete
4.Other crops(Farm)		11.Building	15. School Playground (School)

Table 2. Features for classification

Data	Feature type	Feature	Description
Hyperspectral image	Spectral feature	MNF	Separate noise and signal in image, also reduce the data dimensions of hyperspectral image
		NDVI	Determine the amount of vegetation.
		WBI	Determine the moisture content of the state canopy.
		EVI	Determine the amount of vegetation.
Lidar data	Terrain feature	nDSM	Height of ground surface, can used to distinguish surface objects.
		Roughness	Point cloud dispersion degree at direction of elevation, also indicates the complexity of ground surface.
	Lidar feature	Intensity	Energy of the laser echo
		Echo ratio	The ratio of also indicates the complexity of vertical direction.

3.3 Pixel-based Classification

In pixel-based classification, the Maximum likelihood was used in image classification. The pixel-based classification was according the statistics and features of pixel to identify targets. Because pixel-based analyzed property value individually in pixel level, leading to the result of pixel-based classification had salt and pepper phenomenon obviously. Therefore, In order to reduce salt and pepper phenomenon, the result of pixel-based classification was processed by majority filtering.

3.4 Object-based Classification

In the reality space, the ground surface object was composed by number of pixels. In object-based classification, the segmentation of image aggregates the pixels to image object according to similarity between pixels. For image object, it has both attribute and geometry features, e.g. shape and texture. After segmentation the Nearest neighbor was used to process the object-based classification. The bottom-up method is used for segmentation. This method uses homogeneity index to obtain object. The scale parameter is to control the size of object, and the details of image object are affected by scale parameter.

4. EXPERIMENTAL RESULTS

The experiments include four types of classifications. These are object-based multispectral image classification, pixel-based hyperspectral image classification, object-based hyperspectral image classification, and integration of hyperspectral and lidar object-based classification. These classification methods used same training and test areas for comparison. The training area and test area are manually selected from 50cm aerial orthoimage. The results are presented by overall accuracy and kappa of classification. This study used commercial software, i.e. eCognition^{TM} 8.7 to perform object-based classification. The pixel-based maximum likelihood classification was implemented by ENVI^{TM}. Table 3 showed the comparison of these methods.

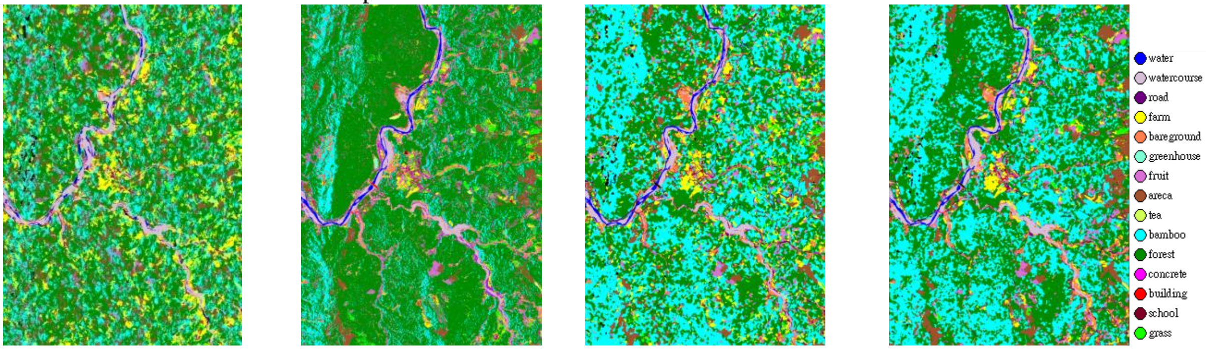

a. object-based mulitispectral image classification

b. pixel-based classification hyperspectral imag

c. object-based hyperspectral image classification

d. integration of hyperspectral image and lidar data for object-based classification

Figure 3. results of classification

4.1 Multispectral vs. hyperspectral image classifications

In this part, Multispectral and hyperspectral images were classified by only spectrum feature. The spectrum feature of multispectral image included four bands, i.e. blue band (450nm), green band (547nm), red band (644nm), near infrared band (780nm) and calculated NDVI, EVI by these four bands. According to the value of spectra and MNF in figure 4, the multispectral image had lower value dispersion degree than hyperspectral MNF image at vegetation. Therefore in Figures 3a and 3c could find the classification in multispectral image had more error than the classification in hyperspectral image at vegetation. In Table 3, the overall accuracy of result of hyperspectral image classification is more accurate than multispectral image classification.

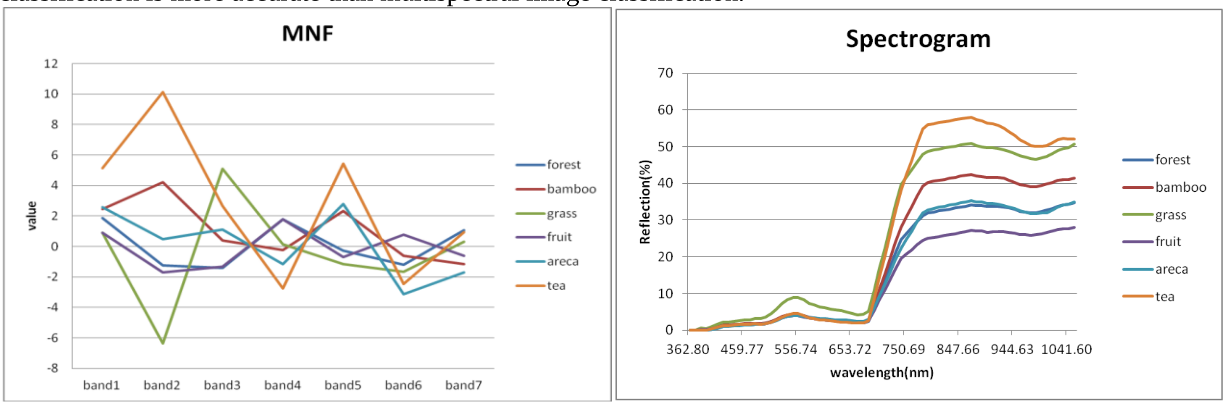

Figure 4. Sperability of landcovers by spectral and MNF

Table 3. Comparison of different approaches

Data	**multispectral image**	**hyperspectral image**	**hyperspectral image**	**hyperspectral image and lidar**
Approach	**object-based**	**pixel-based**	**object-based**	**object-based**
Kappa	0.5062	0.8010	0.9064	0.9554
OA	54.72%	81.77%	91.40%	95.50%

4.2 Pixel-based vs. object-based classifications

The results of pixel-based and object-based classification of hyperspectral image were compared in this section (see figure 5). Because the pixel-based classification classified the land cover using each pixel. The result of pixel-based classification occurred salt and pepper phenomenon significantly. On the other hand, the object-based classification classified the land cover using segmented object. The result showed complete region, e.g. for the fruit plantation and areca plantation in object-based are more complete than pixel-based. Moreover, the pixel-based classification is mixed with other things like grass or broadleaf tree. According to classification accuracy, object-based classification is more helpful than pixel-based classification.

4.3 Image classification with and without lidar features

According to figure 4, tree and areca had similar spectral feature. This phenomenon leaded some misclassifications (see Table 4) like fruit, areca, bamboo and forest etc. The lidar data provide 3D structural features like height and complexity (roughness) for classification. The combination of hyperspectral image and lidar improved the accuracy of classification (see Table 5).

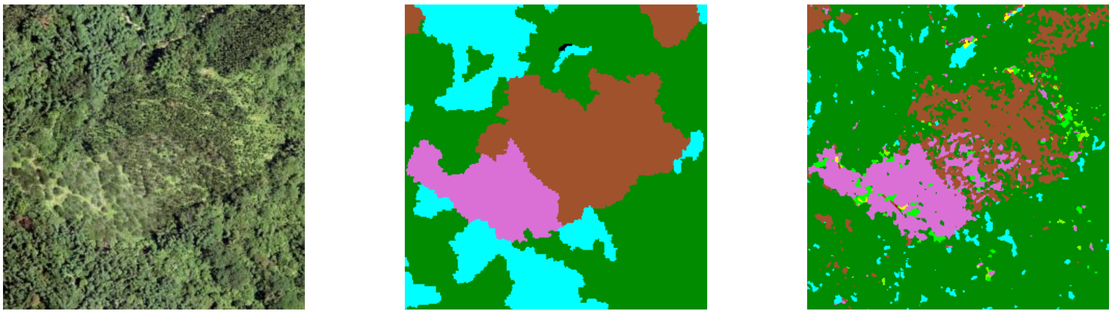

a. Orthophoto b. Object-based classification c. Pixel-based classification

Figure 5. Comparison of object-based classification and pixel-based classification

Table 4. Error matrix for result of hyperspectral object-based classification without lidar data

User \ Reference	water	watercourse	road	farm	bareground	greenhouse	fruit	areca	tea	bamboo	forest	concrete	building	school	grass
water	3398	81	0	0	0	0	0	0	0	0	0	0	0	0	0
watercourse	12	2990	0	0	0	0	0	0	0	0	0	0	0	0	0
road	0	0	2580	0	88	81	0	0	0	0	0	26	58	0	0
farm	0	0	8	2996	54	0	148	0	0	0	258	0	2	55	235
bareground	0	97	36	0	2750	0	6	0	0	0	0	0	0	5	0
greenhouse	0	11	0	0	0	1810	0	0	0	0	0	3	6	0	0
fruit	0	0	0	0	0	0	2290	38	0	0	0	0	0	0	0
areca	0	0	1	26	145	0	0	2878	32	0	151	0	0	0	0
tea	0	0	0	0	0	0	0	0	3127	0	5	0	0	0	0
bamboo	0	0	19	0	12	1	259	364	0	2971	369	0	0	0	1
forest	0	0	3	0	16	0	269	0	0	294	5384	0	0	0	79
concrete	0	0	19	0	0	0	0	0	0	0	0	504	27	0	0
building	0	0	11	0	0	0	0	0	0	0	0	0	1373	0	0
school	0	0	3	0	0	0	0	0	0	0	0	0	3	573	0
grass	0	0	0	179	3	0	0	0	0	0	0	0	0	0	2845
unclassified	0	0	0	0	0	0	0	0	0	0	0	0	21	0	0
Sum	3410	3179	2680	3201	3068	1892	2972	3280	3159	3265	6167	533	1490	633	3160
Producer Acc.	0.9965	0.9405	0.9627	0.9360	0.8963	0.9567	0.7705	0.8774	0.9899	0.9100	0.8730	0.9456	0.9215	0.9052	0.9003
User Acc.	0.9767	0.9960	0.9107	0.7977	0.9502	0.9891	0.9837	0.8902	0.9984	0.7435	0.8907	0.9164	0.9921	0.9896	0.9399
Overall Acc.	0.9140														
K	0.9064														

Table 5. Error matrix for result of hyperspectral object-based classification with lidar data

User \ Reference	water	watercourse	road	farm	bareground	greenhouse	fruit	areca	tea	bamboo	forest	concrete	building	school	grass
water	3391	0	0	0	0	0	0	0	0	0	0	0	0	0	0
watercourse	9	3082	0	0	0	0	0	0	0	0	0	0	0	0	0
road	0	0	2609	0	23	0	0	0	0	0	0	33	129	0	0
farm	0	63	7	3022	3	0	0	0	0	0	14	0	2	0	45
bareground	10	34	9	0	2939	81	0	0	0	0	0	0	3	61	0
greenhouse	0	0	0	0	0	1811	0	0	0	0	0	0	0	0	0
fruit	0	0	0	0	0	0	2947	0	0	0	0	0	0	0	5
areca	0	0	0	0	83	0	0	3092	97	0	1	0	0	0	0
tea	0	0	0	0	0	0	0	0	3037	0	0	0	0	0	0
bamboo	0	0	30	0	7	0	0	104	0	3184	377	0	0	0	0
forest	0	0	0	0	0	0	20	84	0	81	5780	0	0	0	0
concrete	0	0	14	0	0	0	0	0	0	0	0	493	34	0	0
building	0	0	0	0	0	0	0	0	0	0	0	0	1304	0	0
school	0	0	14	0	0	0	5	0	0	0	0	7	7	572	0
grass	0	0	0	179	0	0	0	0	25	0	0	0	0	0	3110
unclassified	0	0	0	0	13	0	0	0	0	0	0	0	11	0	0
Sum	3410	3179	2683	3201	3068	1892	2972	3280	3159	3265	6172	533	1490	633	3160
Producer Acc.	0.9944	0.9695	0.9724	0.9441	0.9580	0.9572	0.9916	0.9427	0.9614	0.9752	0.9365	0.9250	0.8752	0.9036	0.9842
User Acc.	1.0000	0.9971	0.9338	0.9575	0.9369	1.0000	0.9983	0.9447	1.0000	0.8601	0.9690	0.9113	1.0000	0.9455	0.9384
Overall Acc.	0.9590														
K	0.9554														

5. CONCLUSIONS

According to experimental results, hyperspectral image provides detailed spectrum to identify different vegetations when compared to multispectral image. For vegetation which have similar spectral features, we used lidar's surface features to separate vegations. Therefore, the classification with lidar data classified the type of vegetation more accurate. Moreover, the result of object-based classification is a more accuracy than tranditional pixel-based classification. Hence, the object-based classification is more appropriate for the land cover management.

ACKNOWLEDGMENT

The authors would like to thank the Ministry of Interior of Taiwan (project number SYC1030219) for the funding support.

REFERENCES

Ifarraguerri, A., and Chang, C.I., 2000. Unsupervised hyperspectral image analysis with projection pursuit. IEEE Trans. Geoscience and Remote Sensing, 38(6), pp. 2529-2538.

Shaw, G., and Manolakis, D., 2002. Signal processing for hyperspectral image exploitation. Signal Processing Magazine, IEEE, 19(1), pp. 12-16.

Miao, X., Gong, P., Swope, S., Pu, R., Carruthers, R., Anderson, G. L., Heaton, J.S., and Tracy, C. R., 2006. Estimation of yellow starthistle abundance through CASI-2 hyperspectral imagery using linear spectral mixture models. Remote Sensing of Environment, 101(3), pp. 329-341.

Prasad, S., and Bruce, L. M., 2008. Limitations of principal components analysis for hyperspectral target recognition. Geoscience and Remote Sensing Letters, IEEE, 5(4), pp. 625-629.

Xing, J., Bravo, C., Jancsok, P. T., Ramon, H., and De Baerdemaeker, J., 2005. Detecting bruises on ‘Golden Delicious’ apples using hyperspectral imaging with multiple wavebands. Biosystems Engineering, 90(1), pp.27-36.

Guo, L., Chehata, N., Mallet, C., and Boukir, S., 2011. Relevance of airborne lidar and multispectral image data for urban scene classification using Random Forests. ISPRS Journal of Photogrammetry and Remote Sensing, 66(1), pp. 56-66.

Myint, S.W., Gober, P., Brazel, A., Grossman-Clarke, S., and Weng, Q., 2011. Per-pixel vs. object-based classification of urban land cover extraction using high spatial resolution imagery. Remote Sensing of Environment, 115(5), pp. 1145-1161.

Duro, D.C., Franklin, S.E., and Dubé, M.G., 2012. Multi-scale object-based image analysis and feature selection of multi-sensor earth observation imagery using random forests. International Journal of Remote Sensing, 33(14), pp. 4502-4526.

Zhang, C., and Xie, Z., 2012. Combining object-based texture measures with a neural network for vegetation mapping in the Everglades from hyperspectral imagery. Remote Sensing of Environment, 124, pp. 310-320.

Ke, Y., Quackenbush, L.J., and Im, J., 2010. Synergistic use of QuickBird multispectral imagery and LIDAR data for object-based forest species classification. Remote Sensing of Environment, 114(6), pp. 1141-1154.

Höfle, B., and Hollaus, M., 2010. Urban vegetation detection using high density full-waveform airborne lidar data-combination of object-based image and point cloud analysis. In: IAPRS, Vienna, Austria, Vol. XXXVIII, Part 7B, pp. 281-286.

Kim, S., McGaughey, R. J., Andersen, H.E., and Schreuder, G., 2009. Tree species differentiation using intensity data derived from leaf-on and leaf-off airborne laser scanner data. Remote Sensing of Environment, 113(8), pp. 1575-1586.